Effects of Steric Repulsion on Helical Conformation of Poly(*N*-propargylamides) with Phenyl Groups

Jianping Deng, Junichi Tabei, Masashi Shiotsuki, Fumio Sanda, and Toshio Masuda*

Department of Polymer Chemistry, Graduate School of Engineering, Kyoto University, Katsura Campus, Kyoto 615-8510, Japan

Received April 21, 2004; Revised Manuscript Received July 13, 2004

ABSTRACT: *N*-Propargylamides with one, two, and three phenyl groups at the α-position of the carboxyl group [HC≡CCH$_2$NHCOR; **1**, R = C(CH$_3$)$_2$C$_6$H$_5$; **2**, R = CCH$_3$(C$_6$H$_5$)$_2$; **3**, R = C(C$_6$H$_5$)$_3$] were polymerized with a rhodium catalyst, (nbd)Rh$^+$B$^-$(C$_6$H$_5$)$_4$ (nbd = 2,5-norbornadiene), to obtain the corresponding polymers in 85−91% yields. Poly(**1**) possessed a moderate molecular weight (M_n = 6300) and was thoroughly soluble in chloroform and dichloromethane. On the other hand, poly(**2**) and poly(**3**) were not totally soluble in the solvents. The M_n's of chloroform-soluble parts were less than 3000. The secondary structure of these three polymers in chloroform was examined by UV−vis spectroscopy with varying temperature. It was found that only poly(**1**) could adopt helical conformation even at 60 °C. By the copolymerization of either monomer **2** or **3** with HC≡CNH$_2$CO(CH$_2$)$_4$H (**4**), the solubility of the polymers was effectively improved, and the M_n's were remarkably increased. When the content of unit **4** in poly(**2**-*co*-**4**)s was 25% and above, the copolymers could form helical conformation with different degrees, among which poly(**2**$_{0.40}$-*co*-**4**$_{0.60}$) showed the largest helicity. When the content of unit **4** of poly(**3**-*co*-**4**)s exceeded 95%, the copolymer took helical structure partly.

Introduction

Biomacromolecules such as DNA and proteins form the structural basis of life and often adopt helical conformation.[1] The molecular information contained by nucleic acid bases and amino acids ranging from the sequence and hydrophilicity to the chain helicity plays significant roles in determining the high-order structure of biomacromolecules. In addition, the conformational transition of proteins is one of the key factors controlling the activities of living organisms. Stimulated by this elegant strategy of the nature, there has been a continuously growing interest in synthetic polymers that are able to form ordered secondary structure in recent years.[2] Meanwhile, large progress in polymer chemistry makes designing and synthesizing polymers possible, which have the potential to take ordered secondary structure. However, success has been achieved so far only in a limited number of polymers including polymethacrylates,[2b,3] polyisocyanides,[4] polyisocyanates,[5] polysilanes,[6] polyaldehydes,[7] polychlorals,[8] and polyacetylenes.[9] Apart from these polymers, several assembly systems[10] can adopt a helical conformation.

Yashima et al.,[9a−c] Tang et al.,[9d,e] Aoki et al.,[9f] and we[11,12] found that polyacetylenes with appropriate substitutents can adopt helical conformation under certain conditions. Specifically, poly(propiolic esters)[11] form a helix due to steric repulsion between the bulky pendent groups as the predominant driving force. On the other hand, poly(*N*-propargylamides)[12] form a helix based on hydrogen bonds intramolecularly formed between the amide groups in side chains. Additionally, we have recently proposed that steric repulsion should be another key factor deciding the possibility for poly(*N*-propargylamides) to adopt stable helical conformation.[13a,b] In this article, we report the synthesis of novel poly(*N*-propargylamides) bearing one, two, and three phenyl groups at the α-position of the carbonyl group to clarify the effect of bulkiness of the side chains on the higher order structure of the main chains (Scheme 1).

Scheme 1

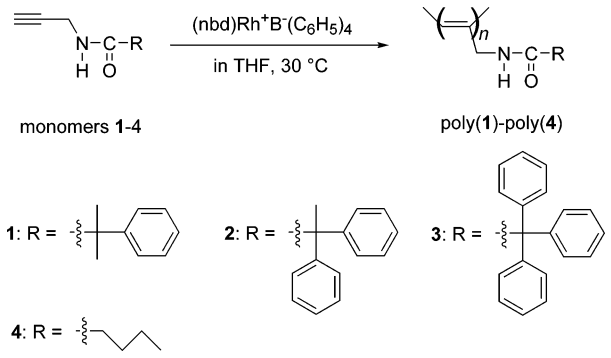

Experimental Section

Measurements. Melting points (mp) were measured by a Yanaco micro melting point apparatus. IR spectra were recorded with a Shimadzu FTIR-8100 spectrophotometer. ^{1}H and ^{13}C NMR spectra were recorded on a JEOL EX-400 spectrometer. Elemental analysis was carried out at the Kyoto University Elemental Analysis Center. Molecular weights and molecular weight distributions of the (co)polymers were determined by GPC (Shodex KF-850 column) calibrated by using polystyrene as standards and $CHCl_3$ as an eluent. UV−vis spectra were recorded on a JASCO J-820 spectropolarimeter.

Materials. THF as polymerization solvent was distilled by the usual method. Propargylamine (TCI), *n*-butyric acid (TCI), 2-phenylisobutyric acid (TCI), 2,2-diphenylpropionic acid (TCI), triphenylacetic acid (TCI), thionyl chloride (Wako), and pyridine (Wako) were used as received. The (nbd)Rh$^+$B$^-$(C$_6$H$_5$)$_4$ catalyst was prepared as reported.[14]

Monomer Synthesis. Monomer **4** was synthesized according to the method reported in a previous article.[13a] Monomers **1**−**3**, which were new compounds, were synthesized according to the method introduced earlier.[12a,13c] Now, taking the synthesis of monomer **1** as an example, the synthetic procedures

* Corresponding author: Tel +81-75-383-2589; Fax +81-75-383-2590; e-mail masuda@adv.polym.kyoto-u.ac.jp.

10.1021/ma0492317 CCC: $27.50
Published on Web 08/25/2004

Table 1. Polymerization of Monomers 1−3[a]

polymer	yield[b] (%)	M_n[c]	M_w/M_n[c]
poly(**1**)	85	6300	2.85
poly(**2**)	90	3000[d]	1.81[d]
poly(**3**)	91	2600[d]	2.41[d]

[a] With (nbd)Rh$^+$B$^-$(C_6H_5)$_4$ as catalyst in THF at 30 °C for 1 h. $[M]_0$ = 0.60 M; $[M]_0$/[Rh] = 100. [b] Hexane-insoluble part. [c] Measured by GPC (polystyrene as standards, $CHCl_3$ as an eluent). [d] The polymer contained $CHCl_3$-insluble part. The data were measured with $CHCl_3$-soluble part after filtration.

are described in detail. 2-Phenylisobutyric acid (5.0 g, 30.0 mmol) was added to thionyl chloride (22.0 mL, 300.0 mmol), and then the resulting solution was refluxed for 3 h. The residual thionyl chloride was removed by rotary pervaporation, ether (200 mL) was added to the residue, and then pyridine (7.8 mL, 90.0 mmol) and propargylamine (6.6 mL, 90.0 mmol) were added sequentially to the solution. The solution was stirred at 0 °C for 2 h, and then white precipitate formed was filtered off. The filtrate was washed with 2 M aqueous HCl three times and then with saturated aqueous $NaHCO_3$ to neutralize the solution. Afterward, the solution was dried over anhydrous $MgSO_4$, filtered, and concentrated to give the target monomer. The crude monomer was purified twice by flash column chromatography on silica gel (hexane/AcOEt = 2.5/1, v/v). Monomers **2** and **3** were prepared in the same way using the corresponding carboxylic acids. The analytical and spectroscopic data of monomers **1**−**3** were as follows:

Monomer **1**: yield 61%, colorless crystal, mp 83−84 °C. IR (KBr): 3294 (H−N), 2360 (H−C≡), 1653 (C═O), 1495, 704 (phenyl), 1529, 1279, 1184, 1008, 654, 540 cm^{-1}. ^{1}H NMR ($CDCl_3$, 400 MHz, 20 °C): δ 1.55 [s, 6H, −CPh(*CH*$_3$)$_2$], 2.10 (s, 1H, *CH*≡C), 3.93 (s, 2H, CH≡C*CH*$_2$), 5.29 (broad s, 1H, N*H*), 7.15−7.20 (m, 5H, Ph−*H*). ^{13}C NMR ($CDCl_3$, 100 MHz, 20 °C): δ 26.97 (×2), 29.44, 46.90, 71.28, 79.51, 126.33 (×2), 127.05, 128.69 (×2), 144.58, 176.98. Anal. Calcd for $C_{13}H_{15}NO$: C, 77.58; H, 7.51; N, 6.96. Found: C, 77.68; H, 7.65; N, 6.93. Monomer **2**: yield 55%, white solid, mp 90−91 °C. IR (KBr): 3242 (H−N), 2112 (H−C≡), 1660 (C═O), 1493, 702 (phenyl), 1269, 1029, 922, 609, 555 cm^{-1}. ^{1}H NMR ($CDCl_3$, 400 MHz, 20 °C): δ 2.03 (s, 3H, CPh$_2$*CH*$_3$), 2.17 (s, 1H, *CH*≡C), 4.03 (s, 2H, CH≡C*CH*$_2$), 5.63 (broad s, 1H, N*H*), 7.30−7.50 (m, 10H, Ph−*H*). ^{13}C NMR ($CDCl_3$, 100 MHz, 20 °C): δ 26.95, 29.64, 56.76, 71.47, 79.31, 127.02 (×2), 128.01 (×4), 128.50 (×4), 144.54 (×2), 174.74. Anal. Calcd for $C_{18}H_{17}NO$: C, 82.10; H, 6.51; N, 5.32. Found: C, 82.03; H, 6.57; N, 5.27. Monomer **3**: yield 57%, white solid, mp 130−131 °C. IR (KBr): 3285 (H−N), 2380 (H−C≡), 1668 (C═O), 1491, 704 (phenyl), 1449, 1226, 1035, 748, 648, 561 cm^{-1}. ^{1}H NMR ($CDCl_3$, 400 MHz, 20 °C): δ 2.14 (s, 1H, *CH*≡C), 4.03 (s, 2H, CH≡C*CH*$_2$), 5.93 (broad s, 1H, N*H*), 7.20−7.35 (m, 15H, Ph−*H*). ^{13}C NMR ($CDCl_3$, 100 MHz, 20 °C): δ 29.80, 67.41, 71.56, 79.18, 127.05 (×3), 127.89 (×6), 130.41 (×6), 142.95 (×3), 173.04. Anal. Calcd for $C_{23}H_{19}NO$: C, 84.89; H, 5.89; N, 4.30. Found: C, 84.77; H, 6.09; N, 4.26.

Polymerization and Copolymerization. (Co)polymerizations were carried out with (nbd)Rh$^+$B$^-$(C_6H_5)$_4$ as a catalyst in dry THF at 30 °C for 1 h under the following conditions: $[monomer]_0$ = 0.60 M, $[monomer]_0$/[catalyst] = 100. After polymerization, the reaction mixture was poured into a large amount of hexane and then (co)polymer precipitated out. Then, the (co)polymer was filtered and dried under reduced pressure. In the case of copolymerization, the total monomer concentration was kept 0.60 M, and the other conditions were the same as those for the homopolymerization.

Molecular Mechanics Calculations. All the calculations were carried out using MMFF94 force field using Spartan'04 Windows version 1.01.

Results and Discussion

Polymer Synthesis. Table 1 shows that monomer **1** underwent polymerization smoothly to give the polymer with a moderate molecular weight (M_n = 6300) in a high yield (85%). On the other hand, poly(**2**) and poly(**3**) contained chloroform-insoluble parts, and so only the molecular weights of chloroform-soluble parts (ca. 70%) could be determined as 2600−3000. It is considered that the chloroform-insoluble parts were polymers with higher molecular weights. Poly(**1**) completely dissolved in chloroform and dichloromethane and partly dissolved in THF, chlorobenzene, and 1,2-dichloroethane; however, poly(**2**) and poly(**3**) were only partly soluble in

Table 2. Solubility of Poly(1)−Poly(3)[a]

solvent	poly(**1**)	poly(**2**)	poly(**3**)
$CHCl_3$	○	□	□
CH_2Cl_2	○	×	×
THF	□	□	□
C_6H_5Cl	□	×	×
toluene	×	×	×
$(CH_2Cl)_2$	□	×	×
DMF	×	×	×
DMSO	×	×	×

[a] ○ = soluble; □ = partly soluble; × = insoluble; the solubility of a polymer sample (2 mg) in a solvent (1 mL) was checked at room temperature. THF = tetrahydrofuran; DMF = *N*,*N*-dimethylformamide; DMSO = dimethyl sulfoxide.

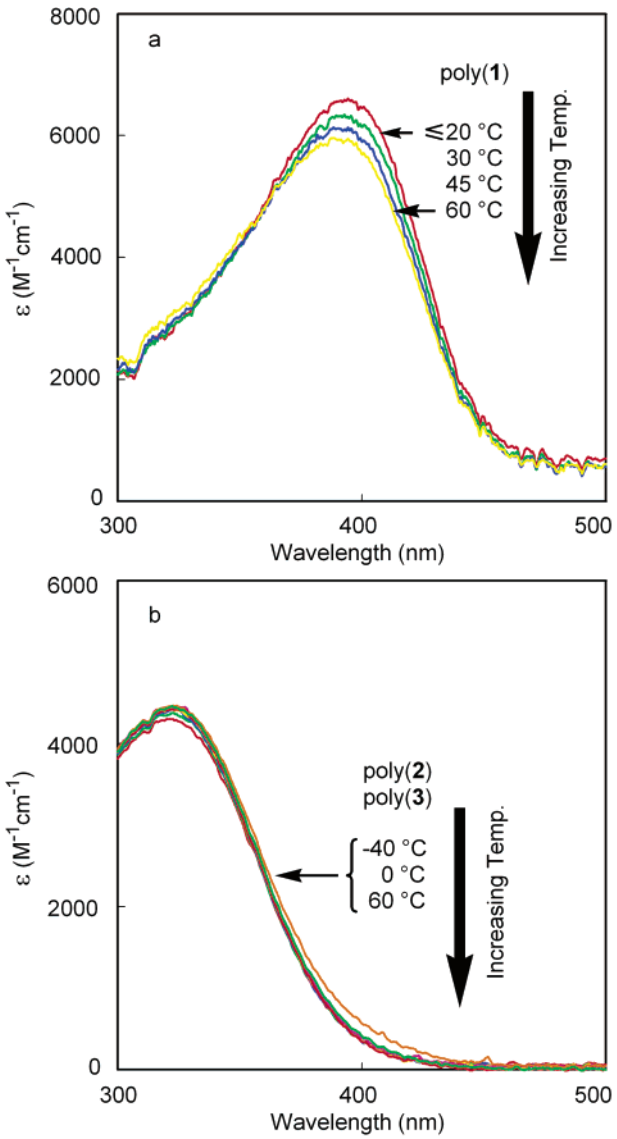

Figure 1. UV−vis spectra of poly(**1**)−poly(**3**) measured in $CHCl_3$ (c = 0.10 mM). The data of poly(**2**) and poly(**3**) were approximate because they were partly (30%) insoluble in $CHCl_3$.

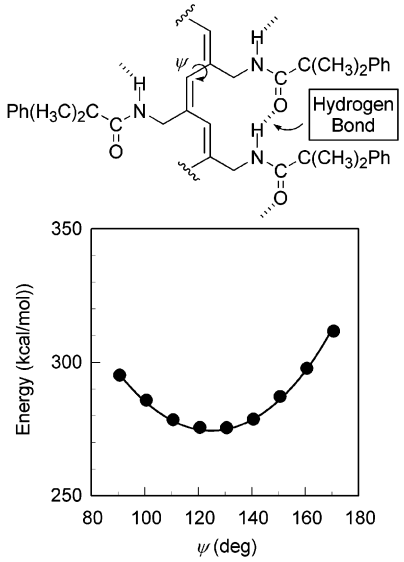

Figure 2. Relationship between the energy and dihedral angle at the single bond of the main chain (ψ) of the 10-mer of **1**. The calculation was carried out by molecular mechanics using the MMFF94 force field.

chloroform and THF, while insoluble in other solvents (Table 2). Precipitates of polymers were observed during the polymerization of **2** and **3**, especially monomer **3**. In addition, the three polymers exhibited very broad ^{1}H NMR signals around 6 ppm in chloroform-*d* at 50 °C, which are assigned to the olefinic protons in the main chain. This can be explained in terms of the bulky phenyl groups, which make the polymer main chains rather stiff and reduce the mobility of the polymer main chains. In fact, the corresponding ^{1}H NMR signal of poly(**4**) was much sharper, whose side chains are sterically less demanding than those of poly(**1**)−poly(**3**).

Secondary Structure of Poly(1)−Poly(3). Our previous research has revealed that poly(*N*-propargylamides) with appropriate substitutents can adopt helical conformation; moreover, both intramolecularly formed hydrogen bonds and steric repulsion between pendent groups are significant factors affecting the stability of the helix.[13] In the current study, the secondary structure of poly(**1**)−poly(**3**) was examined using the soluble parts in chloroform by recording UV−vis spectra at different temperatures, which has been proved to be a simple but effective methodology to investigate the secondary structure of poly(*N*-propargylamides).[12,13] In the UV−vis spectra of poly(**1**) (Figure 1a), only one absorption peak was observed at about 400 nm, while no absorption peak appeared at around 320 nm. According to our earlier studies on the secondary structure of poly(*N*-propargylamides),[12,13] the absorption peak at 390 nm demonstrates the formation of a helix, while the peak at 320 nm corresponds to random coil conformation. It is therefore concluded that poly(**1**) takes a helical conformation in chloroform even at 60 °C, which indicates that the helix is fairly stable at high temperature compared to those in poly(*N*-propargyl-*n*-alkylamides).[13] On the other hand, only one absorption peak appeared around 320 nm in the UV−vis spectra of poly(**2**) and poly(**3**) (Figure 1b). It is concluded that they cannot adopt helical conformation at the temperature range of −40 to 60 °C. In the sequence from poly(**1**) to poly(**3**), steric repulsion between the pendent groups becomes larger, and hence it is assumed that the steric repulsion is appropriate for poly(**1**) to adopt a helix but too large

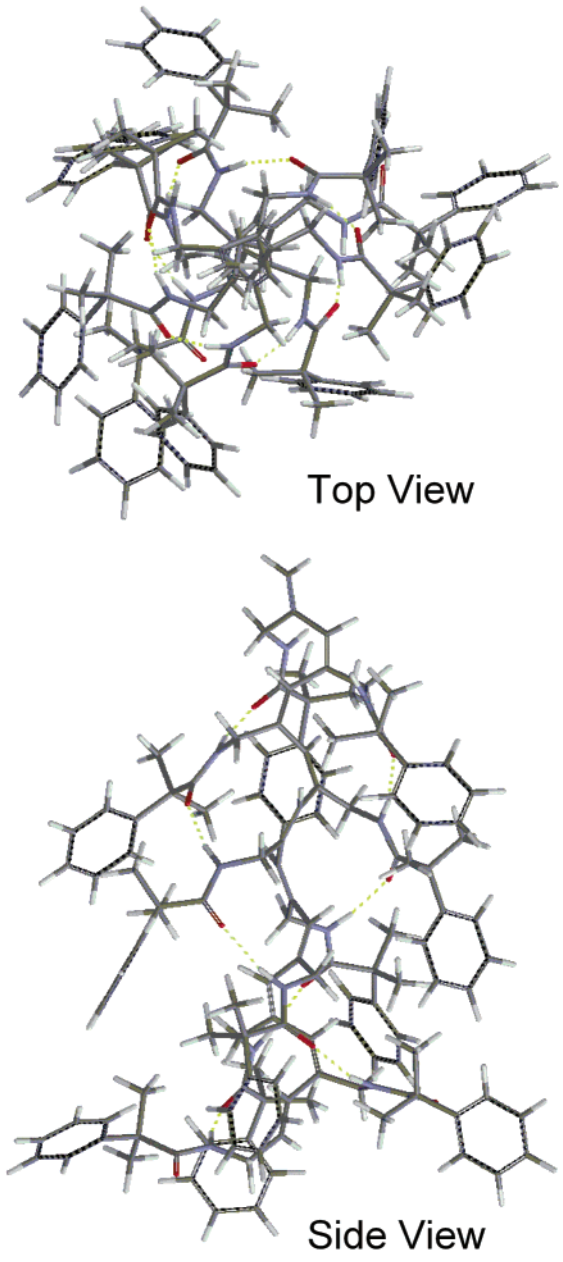

Figure 3. Top and side views of the geometry of 10-mer of **1** optimized by MMFF94. The dihedral angle at the single bond of the main chain (ψ) was fixed at 120°.

in poly(**2**) and poly(**3**), which probably hinders the formation of hydrogen bonds and in turn exerts negative effects on the stability of the helical conformation.

Conformational Analysis by Molecular Mechanics Calculation. Molecular mechanics calculations were carried out to gain information about the reason for the difference of higher order structures of poly(**1**)−poly(**3**), using the MMFF94 force field that can take into account the stabilization effect by hydrogen bonding. Figure 2 depicts the relationship between the dihedral angle at the single bond of the main chain (ψ) and the energy of the 10-mer of **1**, whose both end groups are terminated with hydrogen atoms. The dihedral angle at the double bond of the main chain was fixed at 0°, and ψ was varied from 170° to 90° with 10° decrement. The side chain conformation of the initial geometry was arranged to form hydrogen bonding between the amide groups at *n*th and (n + 2)th units, where the distance between ⟩N−H hydrogen and O═C⟨ oxygen atoms of the

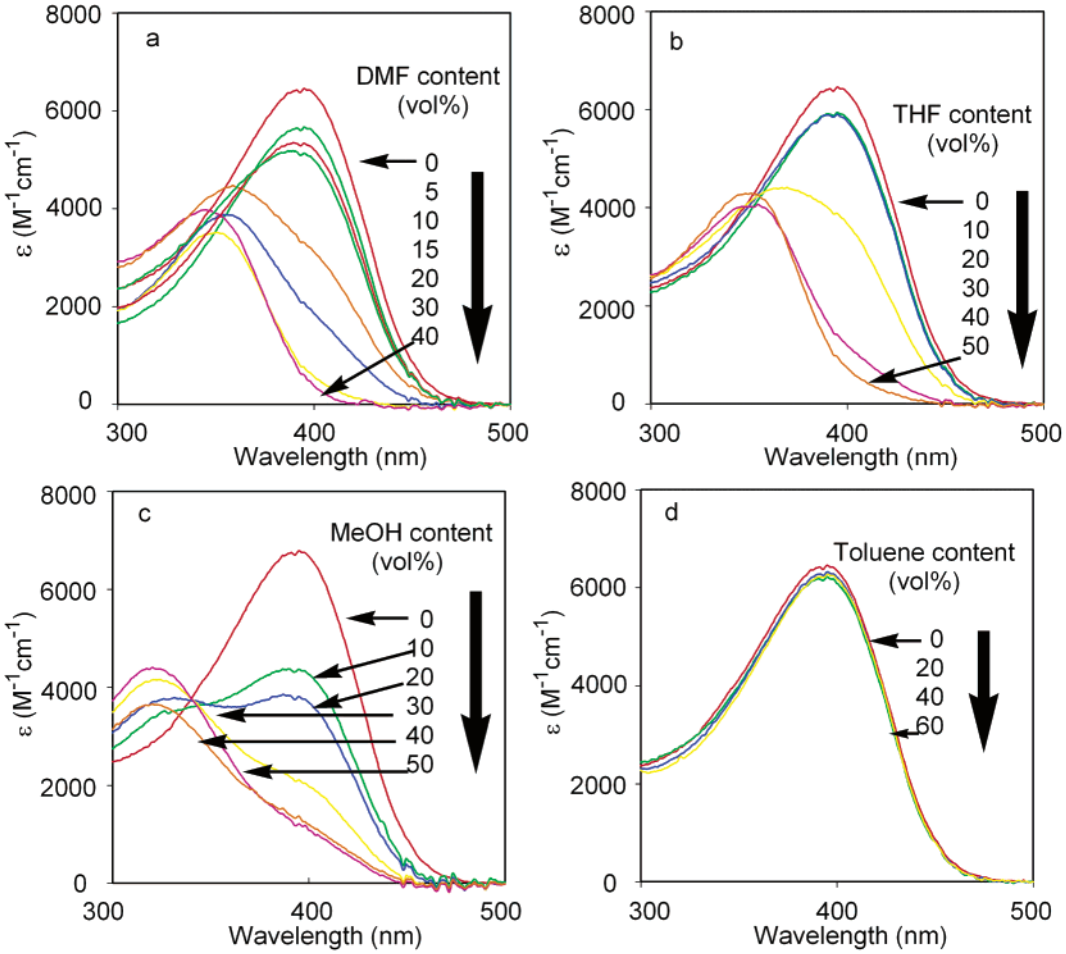

Figure 4. Effects of added solvents on UV−vis spectra of poly(**1**)/$CHCl_3$ at 20 °C (c = 0.10 mM). The total volume of the sample solution was 10 mL.

eight pairs was set at 1.9 Å. Otherwise, all the other geometries were optimized. It was confirmed that the 10-mer of **1** with the dihedral angle of 120°−130° is the most stable among the conformers with ψ ranging from 90° to 170°. The average ⟩N−*H*- - -*O*═C⟨ distance became 1.98 Å after geometry optimization (ψ = 120°), which was almost the same as that of the initial geometry.

The stable geometries of the 10-mers of **2** and **3** were also searched in a manner similar to that of **1**. The 10-mers of **2** and **3** also exhibited the energy minima when ψ was 120°−130°. It should be noted that the average interatomic distance between the ⟩N−H hydrogen and O═C⟨ oxygen atoms of the 10-mers of **2** and **3** became as long as 2.12 and 2.72 Å after geometry optimization, respectively. This result indicates that intramolecular hydrogen bonds tend to break, especially in the 10-mer of **3**. Large steric repulsion between the side chains should be responsible for the fission of hydrogen bonds. It is therefore likely that the bulkiness of the pendent groups of poly(**2**) and poly(**3**) prevents the effective formation of hydrogen bonds for helix formation, and they take a random structure instead.

Figure 3 illustrates the 10-mer of **1** after the geometry was optimized, in which ψ was constrained at 120°. Although the present polymers consist of equivalent amount of right- and left-handed helices, here we assume that poly(**1**) takes right-handed helical structure, wherein all the eight pairs of ⟩N−*H* at *n*th and *O*═C⟨ at (n + 2)th units are located at the positions possibly to form hydrogen bonds (displayed with green dotted lines); i.e., the distance between the hydrogen and oxygen atoms is ranging from 1.6 to 2.1 Å, and the angle of N−H- - -O is larger than 120°. It clearly indicates that the hydrogen bonds between the amide groups at *n*th and (n + 2)th units contribute to the formation of helical structure. On the other hand, the corresponding 10-mers of **2** could form only five hydrogen-bonding pairs due to the repulsion between the bulky pendent groups, and that of **3** could form no pair among the eight pairs of ⟩N−H- - -O═C⟨ possibly to form hydrogen bonds. These results support well the assumption that too bulky pendent groups make the formation of hydrogen bonding disadvantageous.

Effects of Solvents on the Helices Formed in Poly(1). To further elucidate the stability of the helical structure of poly(**1**), several solvents were added to the chloroform solution, and UV−vis spectra were recorded as presented in Figure 4. When DMF was added to the solution, the UV−vis absorption at 390 nm weakened gradually with the increase of DMF, and a new peak appeared simultaneously at about 350 nm. It is considered that DMF destroyed the intramolecular hydrogen bonds between the amide groups in the side chains to a certain degree because DMF can form hydrogen bonds with the amide groups, resulting in the deformation of helical structure. However, a higher order structure should remain because the position of the UV−vis absorption is not at 320 nm (random coil) but at 350 nm, presumably based on another helical structure with

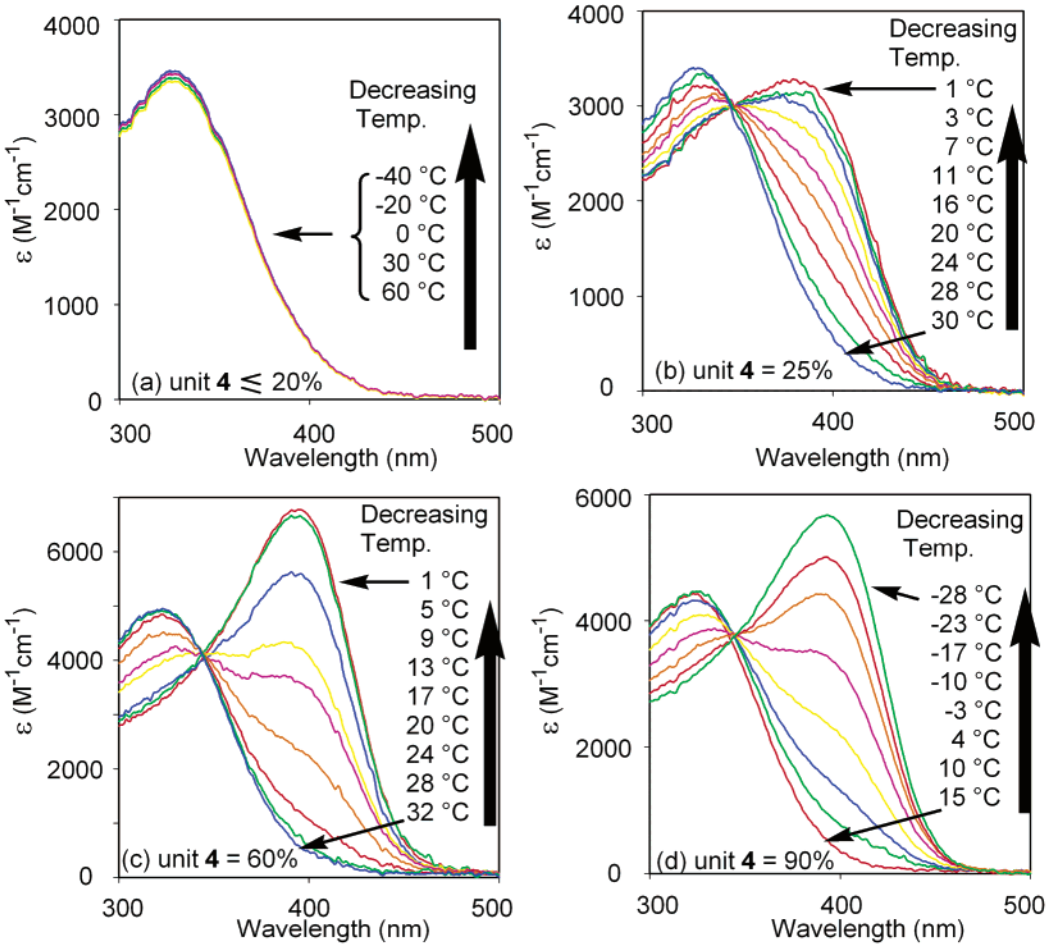

Figure 5. Effects of copolymer composition on the UV−vis spectra of poly(**2**-*co*-**4**)s measured in $CHCl_3$ (c = 0.10 mM) at −45 °C.

Table 3. Copolymerization of Monomers 2 and 4[a]

4 in monomer feed (mol %)	yield[b] (wt %)	M_n[c]	M_w/M_n[c]
0	90	3000	1.81
10	97	4400	1.10
20	98	4700	1.07
25	97	7400	2.03
30	100	6200	2.67
40	99	6010	2.31
50	99	9100	1.68
60	100	9000	1.26
70	98	5200	3.11
80	100	5200	5.09
90	100	6200	3.98
100[d]	80	9500	2.32

[a] With (nbd)$Rh^+B^-(C_6H_5)_4$ as catalyst in THF at 30 °C for 1 h. $[M]_{total}$ = 0.60 M; $[M]_0/[Rh]$ = 100. [b] Hexane-insoluble part. [c] Measured by GPC (polystyrene as standards, $CHCl_3$ as an eluent). [d] With (nbd)$Rh^+B^-(C_6H_5)_4$ as catalyst in THF at 30 °C for 1 h. [M] = 1.0 M; $[M]_0/[Rh]$ = 100.

a different pitch (Figure 4a). Addition of THF gave similar results to the case of DMF as shown in Figure 4b. It is also possible to assume that the UV−vis absorption peak at 350 nm is caused by aggregation of the polymers. However, the UV−vis spectra of the polymer solution were measured again after filtration to find little difference from those before filtration. Thus, this idea is denied.

When methanol was added to the chloroform solution of poly(**1**), the UV absorption at 390 nm gradually weakened and then totally disappeared; in the meantime, absorption at 320 nm gradually increased (Figure 4c), which is different from the cases of DMF and THF. This means that conformational transition took place from helix to random coil, which should stem from the loss of intramolecular hydrogen bonds by added methanol. It can be assumed that methanol, a protic solvent, effectively destroys the intramolecular hydrogen bonds between the amide groups of the side chains compared to DMF and THF, aprotic solvents, but the concrete reason is not clear. Addition of toluene was also examined to find that it hardly affected the helical conformation of the polymer (Figure 4d). On the basis of these results, we can conclude that, even though poly(**1**) carries bulky pendent groups, the hydrogen bonds are affected especially by polar solvents, resulting in the deformation of helical structure.

Synthesis and Secondary Structure of Poly(2-*co*-4)s. Table 3 shows that the copolymerization of monomers **2** and **4** readily proceeded to give the copolymers in high yields (97−100%). All the copolymers possessed moderate molecular weights (4400−9100), and they were totally soluble in chloroform and THF. The ^1H NMR signals assigned to the olefinic protons in the main chain became sharp gradually along with increasing the content of unit **4**; however, the signals were still quite broad compared to that of poly(**4**). Hence, the steric repulsion caused by the pendent groups in monomer **2** may be still large even in the copolymers, and the flexibility of the polymer chain is low.

The UV−vis spectra of poly(**2**-*co*-**4**)s were measured in chloroform. In Figure 5, the spectra of the copolymers containing 20 and below, 25, 60, and 90% of unit **4** are presented as examples. When the content of unit **4** was 20% or smaller, only one absorption peak appeared at

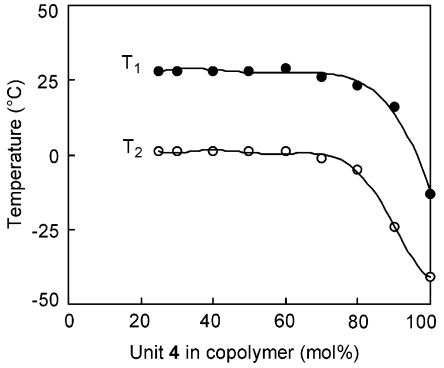

Figure 6. Temperature dependence of UV−vis spectra of poly(**2**-*co*-**4**)s measured in $CHCl_3$ (c = 0.10 mM). T_1 and T_2 are the temperatures at which the coil-to-helix transition begins and ends, respectively.

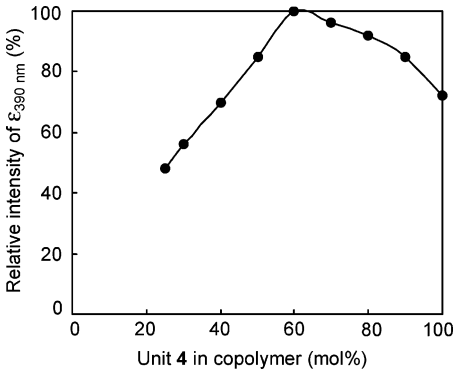

Figure 7. Effects of copolymer composition on the relative intensity of ϵ at 390 nm of poly(**2**-*co*-**4**)s determined by UV−vis spectroscopy measured in $CHCl_3$ (c = 0.10 mM) at −45 °C.

Table 4. Copolymerization of Monomers 3 and 4[a]

4 in monomer feed (mol %)	yield[b] (wt %)	M_n[c]	M_w/M_n[c]
0[d]	91	2600	2.41
20[d]	99	9300	2.27
40	97	22500	1.27
60	98	11000	2.42
80	100	11700	2.73
90	97	10000	2.86
95	98	9400	2.51
100[e]	80	9500	2.27

[a] With (nbd)$Rh^+B^-(C_6H_5)_4$ as catalyst in THF at 30 °C for 1 h. $[M]_{total}$ = 0.60 M; $[M]_0/[Rh]$ = 100. [b] Hexane-insoluble part. [c] Measured by GPC (polystyrene as standards, $CHCl_3$ as an eluent). [d] Partly dissolved in THF and $CHCl_3$. [e] With (nbd)$Rh^+B^-(C_6H_5)_4$ as catalyst in THF at 30 °C for 1 h. [M] = 1.0 M; $[M]_0/[Rh]$ = 100.

around 320 nm above −40 °C, exemplified by the UV−vis spectra in Figure 5a. This indicates that the copolymers bearing low content of unit **4** exists mainly in random coil at the temperature, judging from our previous studies.[13] When the content of unit **4** was 25%, the absorption peak at 320 nm gradually weakened as the temperature was lowered from 30 to 1 °C, and in the meantime, an absorption peak appeared at about 390 nm and became stronger as shown in Figure 5b. This phenomenon became more obvious along with the increase of unit **4** content in the copolymers and demonstrated that more copolymer main chains adopted helical conformation under the examined temperatures. When the content of unit **4** reached 60%, the absorption at 390 nm became the strongest (Figure 5c). The absorption at 390 nm progressively weakened again with further increasing the content of **4** in the copolymers (Figure 5d).

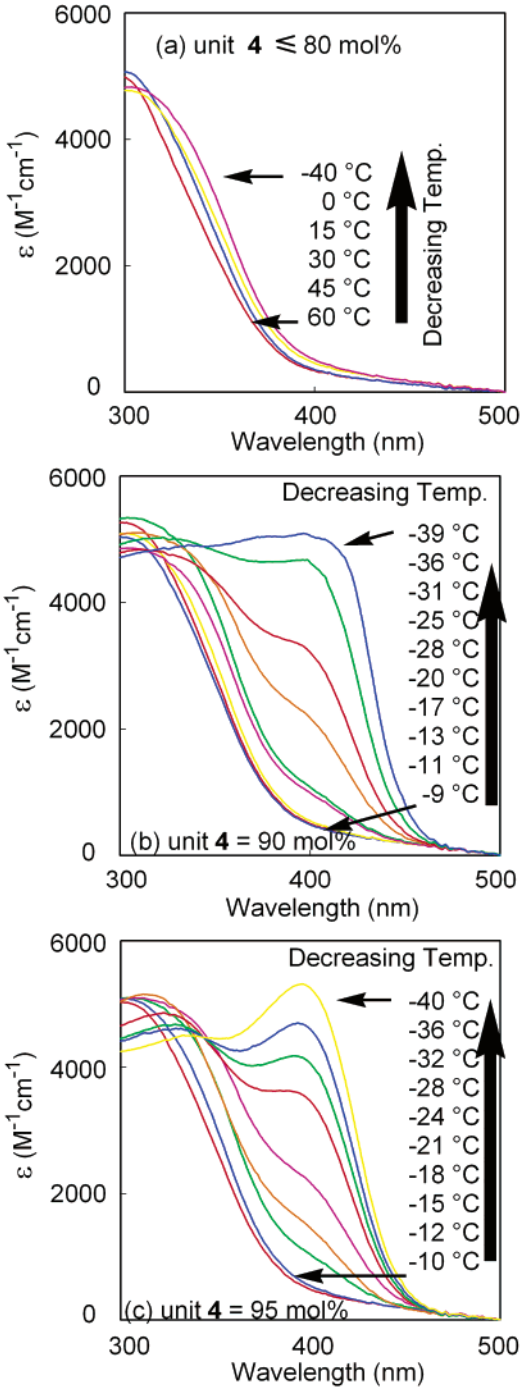

Figure 8. Effects of copolymer composition on the UV−vis spectra of poly(**3**-*co*-**4**)s measured in $CHCl_3$ (c = 0.10 mM).

To understand the results in Figure 5 more clearly, two temperatures are designated as follows: T_1 and T_2 are the temperatures at which the random coil-to-helix transition begins and ends, respectively. Here, it is necessary to point out that the helix content at T_1 is zero, whereas the helix content at T_2 is not necessarily 100% but is a maximum for each (co)polymer under the given conditions.[13] The T_1 and T_2 of these (co)polymers are given in Figure 6. The copolymers previously studied gave maximum T_1 and T_2 at a certain composition,[13b,c] while in the current study, the copolymers with unit **4** smaller than 60% showed almost the same T_1 and T_2 irrespective of the composition (T_1 was about 30 °C and T_2 1 °C). On the other hand, both T_1 and T_2 drastically decreased when the content of unit **4** exceeded 70%. It

is proposed that the large steric repulsion between the crowded pendent groups in unit **2** should be responsible for these results.

Poly($\mathbf{2}_{0.40}$-*co*-$\mathbf{4}_{0.60}$) showed the strongest UV−vis absorption at 390 nm among the copolymers. Therefore, relative intensities of ϵ at 390 nm of the other copolymers to that of poly($\mathbf{2}_{0.40}$-*co*-$\mathbf{4}_{0.60}$) were determined taking this copolymer as a standard based on the earlier calculation methods,[13b,c] and the results are presented in Figure 7. The relative intensities of ϵ at 390 nm in the copolymers linearly increased with increasing the content of unit **4** up to 60%, and then they gradually decreased again as the unit **4** content was raised further. It is suggested from Figure 7 that small steric repulsion between the pendent groups leads to unstable helix in poly(**4**), whereas too bulky pendent groups may prevent the formation of hydrogen bonds and thus place negative influence on the formation of stable helices [poly(**2**)]. Poly($\mathbf{2}_{0.40}$-*co*-$\mathbf{4}_{0.60}$) achieves well the balance between the two types of pendent groups, and therefore this copolymer forms a stable helix.

Synthesis and Secondary Structure of Poly(3-*co*-4)s. The copolymerization of monomers **3** and **4** also underwent satisfactorily to provide the copolymers with moderate M_n's (9300−22 500) in high yields (≥ 97%). The copolymers showed good solubility in chloroform except for poly($\mathbf{3}_{0.80}$-*co*-$\mathbf{4}_{0.20}$). However, the cis content could not be determined by the ^{1}H NMR spectra measured in chloroform-*d* due to broadness of olefinic proton signals.The UV−vis spectra of poly(**3**-*co*-**4**)s were also measured in chloroform. The copolymers did not show absorption at 390 nm even though the content of unit **4** was as large as 80% (Figure 8a). When the content of unit **4** was 90% or higher (Figure 8b,c), poly(**3**-*co*-**4**)s demonstrated some absorption at 390 nm with lowering temperature. However, the absorption at around 320 nm increased only slightly, even though the absorption at 390 nm increased and leveled off with decreasing temperature to −40 °C. These results are quite different from those in poly(**2**-*co*-**4**)s (Figure 5), which should be due to the difference of steric repulsion between the pendent groups in poly(**2**) and poly(**3**). Specifically, poly(**2**) possesses large steric repulsion, but the steric repulsion can be decreased appropriately and effectively by the copolymerization with monomer **4**. On the other hand, poly(**3**) possesses so large pendent groups that the steric repulsion between the pendent groups still restricts the formation of effective hydrogen bonds even in the copolymers with monomer **4**, which is indispensable for the polymers to adopt a stable helix.

Conclusions

Novel *N*-propargylamides **1**−**3** with one, two, or three phenyl groups at the α-position of the carbonyl group were synthesized. Among the three monomers, monomer **1** with the smallest substitutent smoothly polymerized to provide poly(**1**) with moderate molecular weight and good solubility in chloroform. However, monomers **2** and **3** with larger substitutents gave polymers with low solubility. Poly(**1**) adopted a relatively stable helix even at high temperatures up to 60 °C, while poly(**2**) and poly(**3**) did not take a helical conformation under the examined conditions. By the copolymerization with *N*-propargylpentanamide **4**, poly(**2**-*co*-**4**)s could adopt helical conformation when the content of unit **4** exceeded 25%; poly($\mathbf{2}_{0.40}$-*co*-$\mathbf{4}_{0.60}$) showed the highest helix content among the copolymers. On the other hand, poly(**3**-*co*-**4**)s could not form stable helical conformation under the same conditions. Accordingly, it is concluded that the pendent groups with appropriate bulkiness are favorable for the polymers to adopt stable helical conformation, and too bulky pendent groups exert negative effects on the formation of a stable helix.

References and Notes

(1) (a) Mason, S. F. *Chiral Evolution: Origin of the Elements, Molecules, and Living Systems*, 2nd ed.; Oxford University Press: London, 1991. (b) Pfeil, W. *Protein Stability and Folding: A Collection of Thermodynamic Data*; Springer-Verlag: Berlin, 1998. (c) Alaos, M.; Babiano, R.; Cintas, P.; Jimenez, J. L.; Palacios, J. C.; Barron, L. D. *Chem. Rev.* **1998**, *98*, 2391−2404.

(2) For the synthetic helical polymers, see: (a) Yashima, E.; Maeda, K.; Nishimura, T. *Chem.—Eur. J.* **2004**, *10*, 42−51. (b) Nakano, T.; Okamoto, Y. *Chem. Rev.* **2001**, *101*, 4013−4038. (c) Green, M. M.; Park, J.-W.; Sato, T.; Teramoto, A.; Lifson, S.; Selinger, R. L. B.; Selinger, J. V. *Angew. Chem., Int. Ed.* **1999**, *38*, 3138−3154. (d) Rowan, A. E.; Nolte, R. J. M. *Angew. Chem., Int. Engl.* **1998**, *37*, 63−68. (e) Pu, L. *Acta Polym.* **1997**, *48*, 116−141.

(3) (a) Okamoto, Y.; Nakano, T. *Chem. Rev.* **1994**, *94*, 349−372. (b) Okamoto, Y.; Suzuki, K.; Ohta, K.; Hatada, K.; Yuki, H. *J. Am. Chem. Soc.* **1979**, *101*, 4763−4765.

(4) (a) Ito, Y.; Ohara, T.; Shima, R.; Suginome, M. *J. Am. Chem. Soc.* **1996**, *118*, 9188−9189. (b) Takei, F.; Yanai, K.; Onitsuka, K.; Takahashi, S. *Angew. Chem., Int. Ed. Engl.* **1996**, *35*, 1554−1555.

(5) (a) Jha, S. K.; Cheon, K. S.; Green, M. M.; Selinger, J. V. *J. Am. Chem. Soc.* **1999**, *121*, 1665−1673. (b) Okamoto, Y.; Matsuda, M.; Nakano, T.; Yashima, E. *J. Polym. Sci., Part A: Polym. Chem.* **1994**, *32*, 309−315.

(6) (a) Nakashima, H.; Fujiki, M.; Koe, J. R. *Macromolecules* **1999**, *32*, 7707−7709. (b) Fujiki, M. *J. Am. Chem. Soc.* **1994**, *116*, 11976−11981.

(7) Choi, S.-H.; Yashima, E.; Okamoto, Y. *Macromolecules* **1996**, *29*, 1880−1885.

(8) Ute, K.; Hirose, K.; Kashimoto, H.; Hatada, K.; Vogel, O. *J. Am. Chem. Soc.* **1991**, *113*, 6305−6306.

(9) (a) Nonokawa, R.; Oobo, M.; Yashima, E. *Macromolecules* **2003**, *36*, 6599−6606. (b) Maeda, K.; Goto, H.; Yashima, E. *Macromolecules* **2001**, *34*, 1160−1164. (c) Maeda, K.; Okada, S.; Yashima, E.; Okamoto, Y. *J. Polym. Sci., Part A: Polym. Chem.* **2001**, *39*, 3180−3189. (d) Li, B. S.; Cheuk, K. K. L.; Ling, L.; Chen, J.; Xiao, X.; Bai, C.; Tang, B. Z. *Macromolecules* **2003**, *36*, 77−85. (e) Li, B. S.; Cheuk, K. K. L.; Salhi, F.; Lam, J. W. Y.; Cha, J. A. K.; Bai, C. L.; Tang, B. Z. *Nano Lett.* **2001**, *1*, 323−328. (f) Aoki, T.; Kaneko, T.; Maruyama, N.; Sumi, A.; Takahashi, M.; Sato, T.; Teraguchi, M. *J. Am. Chem. Soc.* **2003**, *125*, 6346−6347.

(10) (a) Prince, R. B.; Brunsveld, L.; Meijer, E. W.; Moore, J. S. *Angew. Chem., Int. Ed.* **2000**, *39*, 228−230. (b) Cuccia, L. A.; Lehn, J. M.; Homo, J. C.; Schmutz, M. *Angew. Chem., Int. Ed.* **2000**, *39*, 233−237.

(11) (a) Nakako, H.; Nomura, R.; Tabata, M.; Masuda, T. *Macromolecules* **2001**, *34*, 1496−1502. (b) Nomura, R.; Fukushima, Y.; Nakako, H.; Masuda, T. *J. Am. Chem. Soc.* **2000**, *37*, 8830−8831. (c) Nakako, H.; Mayahara, Y.; Nomura, R.; Tabata, M.; Masuda, T. *Macromolecules* **2000**, *33*, 3978−3982. (d) Nakako, H.; Nomura, R.; Tabata, M.; Masuda, T. *Macromolecules* **1999**, *32*, 2861−2864.

(12) (a) Tabei, J.; Nomura, R.; Sanda, F.; Masuda, T. *Macromolecules* **2003**, *36*, 8603−8608. (b) Nomura, R.; Nishiura, S.; Tabei, J.; Sanda, F.; Masuda, T. *Macromolecules* **2003**, *36*, 5076−5080. (c) Nomura, R.; Tabei, J.; Nishiura, S.; Masuda, T. *Macromolecules* **2003**, *36*, 561−564. (d) Tabei, J.; Nomura, R.; Masuda, T. *Macromolecules* **2002**, *35*, 5405−5409. (e) Nomura, R.; Tabei, J.; Masuda, T. *Macromolecules* **2002**, *35*, 2955−2961. (f) Nomura, R.; Tabei, J.; Masuda, T. *J. Am. Chem. Soc.* **2001**, *123*, 8430−8431.

(13) (a) Deng, J.; Tabei, J.; Shiotsuki, M.; Sanda, F.; Masuda, T. *Macromolecules* **2004**, *37*, 1891−1896. (b) Deng, J.; Tabei, J.; Shiotsuki, M.; Sanda, F.; Masuda, T. *Macromol. Chem. Phys.* **2004**, *205*, 1103−1107. (c) Deng, J.; Tabei, J.; Shiotsuki, M.; Sanda, F.; Masuda, T. *Macromolecules* **2004**, *37*, 5149−5154.

(14) Schrock, R. R.; Osborn, J. A. *Inorg. Chem.* **1970**, *10*, 2339−2343.

MA0492317